Annual Reviews in Control 000 (2015) 1–11

Contents lists available at ScienceDirect

Annual Reviews in Control

journal homepage: www.elsevier.com/locate/arcontrol

Fault-tolerant control of wind turbines with hydrostatic transmission using Takagi–Sugeno and sliding mode techniques☆

Horst Schulte*, Eckhard Gauterin

HTW University of Applied Sciences Berlin, Department of Engineering I, Control Engineering Group, Wilhelminenhofstr. 75a, Berlin D-12459, Germany

ARTICLE INFO

Article history:
Received 15 June 2015
Accepted 2 August 2015
Available online xxx

Keywords:
Wind turbine control
Fault tolerant Control
Sliding-mode observer
Takagi–Sugeno systems

ABSTRACT

In this paper, a Takagi–Sugeno Sliding Mode Observer for actuator fault diagnosis and fault-tolerant control scheme of wind turbines with hydrostatic transmission are presented. It will be shown that sliding mode techniques have the advantages that several actuator faults of the wind turbine drive train can be simultaneously reconstructed with one and the same observer and directly applied for fault compensation. Furthermore, a simple compensation approach is implemented by subtracting the reconstructed faults obtained from the (faulty) inputs. These corrected inputs act on the system as virtual actuators, such that the originally designed controller for the nominal, i.e. fault-free situation, can still be used. The fault reconstruction and fault tolerant control strategy are tested in simulations with several faults of different types.

1. Introduction

Wind turbines with hydrostatic transmission are not yet available in commercial systems. Only recently, however, this drive train concept has been considered as an alternative to conventional wind turbines. There are several reasons for this: firstly over the rated power range between 1.5 and 10 MW, the existing gear-less direct-drive concepts cause an increase of weight around 25 percent and a cost increase of around 30 percent (Ragheb & Ragheb, 2010). Secondly, the conventional gearboxes of modern wind turbines at the Mega-Watt (MW) level of rated power are highly stressed by different load cases, where wind gusts and turbulence lead to misalignment of the drive train and a gradual failure of the gear components. This failure interval creates a significant increase in the capital and operating costs and downtime of a turbine, while greatly reducing its profitability and reliability (Ragheb & Ragheb, 2010).

In contrast, hydrostatic transmission allows mechanically decoupled operation of wind turbine rotor and generator over a wider range of wind speeds without the need of mechanical gearboxes and frequency converters. It permits the use of synchronous generators with low numbers of poles, which are cheaper than double fed induction generator for indirect drive (with gearbox) and multi-pole synchronous generators for direct drive (without gearboxes). Both drive-train configurations are commonly used in variable speed machines today. Furthermore, as a consequence of the omission of power electronics, the use of synchronous generator with an electrical voltage up to a range of 10 kV eliminates the need for voltage transformer. According to the investigation in Diepeveen and Laguna (2011), hydrostatic transmission also have a positive impact on power quality, since small rotor speed fluctuations due to wind gusts are absorbed.

Up to now, hydraulic transmissions are mainly used in construction and agricultural equipment. For these kinds of applications, condition monitoring, fault diagnosis and maintenance are easy to perform. However, for a reliable operation of hydrostatic transmission in wind turbines, fault diagnosis and fault tolerant control are indispensable especially for offshore applications. Only a few model-based fault-tolerant control approaches exist for wind turbines with conventional drive-trains. In Sloth, Esbensen, and Stoustrup (2011), passive and active fault-tolerant controllers are designed and considered with regard to accommodating altered actuator dynamics in the pitch system model. In Odgaard and Stoustrup (2012), a bank of unknown-input observers is used for fault diagnosis in the rotor and generator speed sensors of the fault detection isolation (FDI) benchmark model presented in Odgaard, Stoustrup, and Kinnaert (2009). In Sami and Patton (2012b), Sami and Patton (2014) active fault-tolerant control is achieved in the partial-load region of wind turbines by means of a sensor fault hiding approach. The fault-tolerant control (FTC) strategy uses a multiple integral observer and a fast adaptive fuzzy estimator, where the observer designs are based on a nonlinear Takagi–Sugeno (TS) model. In Sami and Patton (2012a), a passive sensor fault-tolerant control strategy is implemented using a sliding mode controller for the partial-load region that tolerates generator speed sensor faults and generator torque offset faults. In Rotondo, Puig, Valle, and Nejjari (2013), an FTC strategy using Linear Parameter Varying (LPV) virtual

☆ A shorter version of this paper was presented at the 19th IFAC World Congress, Cape Town, South Africa, August 24-29, 2014

* Corresponding author.
E-mail addresses: horst.schulte@htw-berlin.de (H. Schulte), eckhard.gauterin@htw-berlin.de (E. Gauterin).

http://dx.doi.org/10.1016/j.arcontrol.2015.08.003
1367-5788/

sensors is proposed and applied to the benchmark model (Odgaard et al., 2009). Instead of hiding the fault, the virtual sensor is used to expand the set of available sensors before the state observer is designed. In Simani and Castaldi (2014), an FTC scheme based on adaptive filters obtained via the nonlinear geometric approach is applied to the actuator of a wind turbine benchmark model. It is shown that the proposed approach allows us to obtain an interesting decoupling property with respect to uncertainty affecting the wind turbine system. A fuzzy modeling and identification method for fault detection and FTC is applied in Badihi, Zhang, and Hong (2014). The proposed fuzzy gain-scheduled fault-tolerant control system is evaluated by a series of simulations on a wind turbine benchmark in the presence different fault scenarios. In Badihi, Zhang, and Hong (2015), the method of Badihi et al. (2014) is compared with a fuzzy model-reference adaptive control in which a fuzzy inference mechanism is used for parameter adaptation without any explicit knowledge of the system faults. In Georg and Schulte (2013), a Takagi–Sugeno sliding mode observer (TS SMO) is used to reconstruct actuator and sensor faults in wind turbines with conventional drive train. Here, the proposed FTC strategy is based on the modification of the control inputs in the presence of actuator faults and on the active-fault compensation of the sensor output signal in the presence of sensor faults. Both strategies serve a behavior similar to the fault-free case.

In this paper, a TS SMO for actuator fault diagnosis and fault-tolerant control scheme for wind turbines with hydrostatic transmission is presented. It will be shown that TS SMO has the advantages that several faults in the two different actuators (hydraulic pump and hydraulic motor) of the wind turbine drive train can be reconstructed with one and the same observer and directly applied for fault compensation. In this work, a simple compensation approach is implemented by subtracting the reconstructed faults obtained from the (faulty) inputs. These corrected inputs act on the system as virtual actuators, such that the originally designed controller for the nominal, i.e. fault-free situation, can still be used.

This paper is organized as follows: Section 2 presents a control-oriented nominal model in Takagi–Sugeno form as an exact representation of a holistic nonlinear physical model of a horizontal axes wind turbine with hydrostatic transmission. A nominal controller strategy is proposed in Section 3. The objective is a fixed, wind speed independent rated speed of the synchronous generator. For this, the rotor/generator speed ratio is continuously adjusted by a variable-displacement hydraulic pump and motor. In Section 4, the observer-based method for fault diagnosis is described. In particular, the TS SMO structure and design for directly reconstruction of faults is briefly introduced. After, the fault tolerant control strategy for actuator faults are introduced and tested in simulations. Finally, a conclusion and an overlook on possible future work are given in Section 5.

2. Control-oriented modeling

In the following the operation principle of hydrostatic transmission in wind turbines is briefly described and a holistic control-oriented model of the overall system in Takagi–Sugeno's form is proposed. A detailed derivation of the wind turbine model using TS model structure is given in Georg, Schulte, and Aschemann (2012). The novel drive train concept is described and published in the recent work (Schulte, 2014). It must be pointed out, that the collective pitch angle is not considered as a control input, because the focus is on the fault tolerant speed control of the generator and the optimal control in the partial load, such that the rotor is constantly running around the optimal tip speed ratio. Nevertheless, the pitch angle in the control-oriented model may considered as a measurable premise variable for the transition between partial and full load range.

2.1. Wind turbine with hydrostatic transmission

In contrast to wind turbines with conventional drive trains, the inertia power in hydrostatic transmissions is transmitted by static oil pressure and flow rate. One advantage is that the transmission ratio between rotor and generator is continuously adjustable. The entire drive train consists of the low speed shaft (LSS), the high speed shaft (HSS) and the hydrostatic transmission line. In its simplest form, the hydrostatic transmission consists of a hydraulic pump and motor, of which at least one must have a variable displacement. A configuration with a variable pump and a variable motor is illustrated in Fig. 1. Other configurations are investigated in Skaare, Nielsen, and Hörnsten (2013), with a variable displacement pump and fixed motor and in Dolan and Aschemann (2012) with a fixed pump and a variable displacement motor.

On the transmission input side, the torque and speed of the rotor are converted by the hydraulic pump into a pressurized oil flow q_P. On the output side, the pressurized flow q_M is converted back into mechanical torque and speed by the hydraulic motor. By varying the displacement of the hydraulic components, any desired transmission ratio can be adjusted. This can be illustrated by the following considerations: The fluid flow q_P produced by the pump is proportional to its rotational speed n_P and depends on the variable volume of the pump per revolution. Indeed, the volume is not constant and proportional to the normalized position $\tilde{x}_P$ of the displacement unit

$$q_P = V_P\, \tilde{x}_P\, n_P \quad \text{with} \quad \tilde{x}_P = x_P / x_{P_{max}} \leq 1 \tag{1}$$

where V_P is the maximum volumetric displacement per revolution of the pump. Similarly, the volume flow through the hydraulic motor is given by

$$q_M = V_M\, \tilde{x}_M\, n_M \quad \text{with} \quad \tilde{x}_M = x_M / x_{M_{max}} \leq 1 \tag{2}$$

where $\tilde{x}_M$ denotes the normalized position of the displacement unit, and n_M the rotational speed of the motor shaft. Fig. 1 shows that the pump feeds directly the motor. Neglecting the compressibility of the fluid and hydrostatic losses it holds that $q_P = q_M$ and with (1), (2) we obtain

$$r_{cv}(\tilde{x}_P, \tilde{x}_M) = \frac{n_M}{n_P} = \frac{V_P}{V_M}\,\frac{\tilde{x}_P}{\tilde{x}_M}\,. \tag{3}$$

That is, the continuously variable transmission ratio r_{cv} depends on the constant ratio $\frac{V_P}{V_M}$ of the maximum volumetric displacement of the pump/motor combination and the adjustable ratio of the position $\tilde{x}_P$ and $\tilde{x}_M$. Thereby the maximum transmission ratio $r_{cv,\,max}$ results from maximum normalized position of the pump displacement $\tilde{x}_P = 1$ and the minimum normalized position of the motor displacement with $\tilde{x}_M \ll 1$.

The necessary high transmission ratio for wind turbines of the Megawatt class up to 2.5 MW can easily be reached by a suitably large ratio of the maximum volumetric displacements V_P/V_M. By taking advantage of the second adjustable term $\tilde{x}_P/\tilde{x}_M$, the transmission ratio can be varied in such a way that the generator operates at constant speed directly connected to the electric grid.

2.2. Takagi–Sugeno model representation

In the next step a Takagi–Sugeno model of the entire wind turbine system will be derived using the sub-models of the wind turbine mechanics (Georg et al., 2012), the hydrostatic transmission (Schulte & Gerland, 2010), the aero map C_Q for rotor torque calculation T_r and the reduced model of the hydraulic pump and motor with a first order delay model of the displacement units. The nonlinear state space model of a wind turbine with hydrostatic transmission is thus given by

$$\dot{\omega}_r = \frac{1}{J_r}\left(T_r(\lambda, \beta) - \tilde{V}_P\, \tilde{x}_P\, \Delta p\right)$$

Please cite this article as: H. Schulte, E. Gauterin, Fault-tolerant control of wind turbines with hydrostatic transmission using Takagi–Sugeno and sliding mode techniques, Annual Reviews in Control (2015), http://dx.doi.org/10.1016/j.arcontrol.2015.08.003

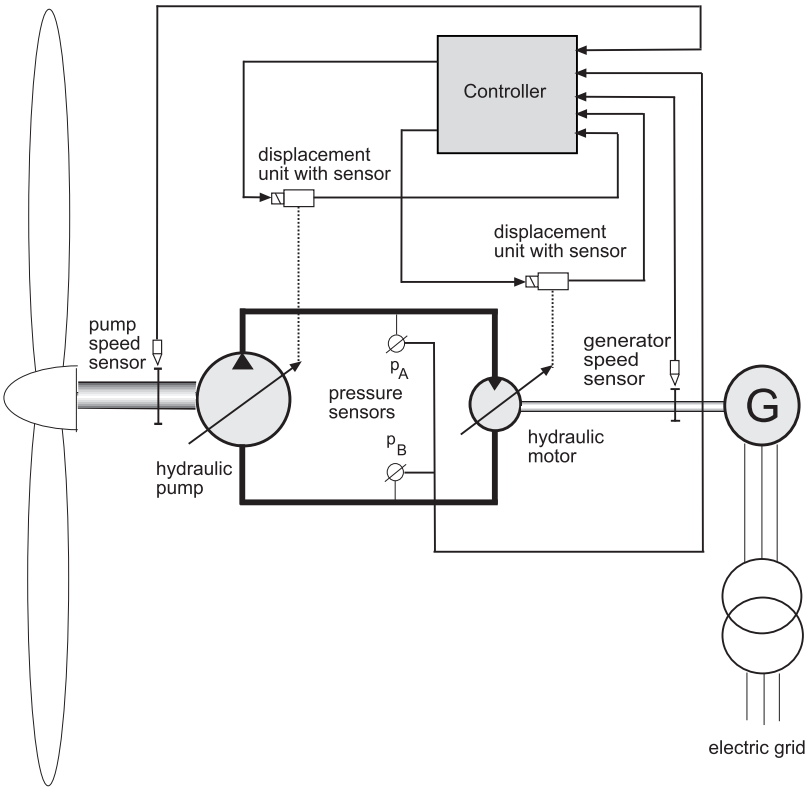

Fig. 1. Simplified hydrostatic drive train schematic.

$$
\begin{aligned}
\dot{\omega}_g &= \frac{1}{J_g}(\tilde{V}_M\,\tilde{x}_M\,\Delta p - T_g)\\
\Delta\dot{p} &= \frac{1}{C_H}\left(\tilde{V}_P\,\tilde{x}_P\,\omega_r - \tilde{V}_M\,\tilde{x}_M\,\omega_g - k_{\text{leak}}\,\Delta p\right)\\
\dot{T}_g &= -\frac{1}{\tau_g}\,T_g + \frac{1}{\tau_g}\,T_{g,d}\\
\dot{\tilde{x}}_P &= -\frac{1}{\tau_P}\,\tilde{x}_P + \frac{1}{\tau_P}\,u_P\\
\dot{\tilde{x}}_M &= -\frac{1}{\tau_M}\,\tilde{x}_M + \frac{1}{\tau_M}\,u_M
\end{aligned}
\tag{4}
$$

with $\tilde{V}_{P,M} = \frac{V_{P,M}}{2\pi}$, the inputs $\mathbf{u} = [\,T_g \quad u_P \quad u_M\,]^T$, the states

$$\mathbf{x} = [\omega_r \quad \omega_g \quad \Delta p \quad T_g \quad \tilde{x}_P \quad \tilde{x}_M]^T$$

and outputs $\mathbf{y} = [\omega_r \quad \omega_g \quad T_g \quad \tilde{x}_P \quad \tilde{x}_M]^T$ where ω_r denotes the rotor angular velocity, ω_g denotes the generator angular velocity, $\Delta p = p_A - p_B$ is the difference between the hydraulic line A and B, see Fig. 1 and T_g as the generator torque and $T_{g,d}$ as the demanded generator torque. The model parameters are J_r and J_g as the rotor and generator inertia, C_H as the hydraulic capacitance, k_{leak} as the lumped leakage coefficient and τ_g, τ_M and τ_P as the delay time constant for generator torque, pump displacement and motor displacement dynamics. The rotor torque depends on the pitch angle β, the wind speed v and the rotor speed

$$T_r = \frac{1}{2}\,\rho_{air}\,\pi\,R^3\,v^2\,C_Q(\lambda,\beta) \tag{5}$$

with the tip speed ratio $\lambda = \frac{\omega_r R}{v}$, where ρ_{air} denotes the air density and R as the rotor radius. It should be pointed out that the use of Takagi–Sugeno (TS) model structure provides a way to obtain an exact representation of the full nonlinear model (4) as a weighted combination of linear sub-models, where the nonlinearities of the system are shifted into weighting functions also called membership functions.

For the conversion into a Takagi–Sugeno model, the following nonlinear functions are defined

$$f_1(\lambda,\beta) = \frac{T_r(\lambda,\beta)}{\omega_g}, \qquad f_2(\tilde{x}_P) = \tilde{x}_P, \qquad f_3(\tilde{x}_M) = \tilde{x}_M \tag{6}$$

such that (4) can be rearranged as

$$
\dot{\mathbf{x}} = \underbrace{\begin{bmatrix} 0 & a_{12} & a_{13} & 0 & 0 & 0\\ 0 & 0 & a_{23} & -\frac{1}{J_g} & 0 & 0\\ a_{31} & a_{32} & -\frac{k_{leak}}{C_H} & 0 & 0 & 0\\ 0 & 0 & 0 & -\frac{1}{\tau_g} & 0 & 0\\ 0 & 0 & 0 & 0 & -\frac{1}{\tau_{x_P}} & 0\\ 0 & 0 & 0 & 0 & 0 & -\frac{1}{\tau_{x_M}} \end{bmatrix}}_{\mathbf{A}(\lambda,\beta)} \underbrace{\begin{bmatrix} \omega_r\\ \omega_g\\ \Delta p\\ T_g\\ \tilde{x}_P\\ \tilde{x}_M \end{bmatrix}}_{\mathbf{x}} + \underbrace{\begin{bmatrix} 0 & 0 & 0\\ 0 & 0 & 0\\ 0 & 0 & 0\\ 0 & 0 & \frac{1}{\tau_g}\\ \frac{1}{\tau_P} & 0 & 0\\ 0 & \frac{1}{\tau_M} & 0 \end{bmatrix}}_{\mathbf{B}} \underbrace{\begin{bmatrix} u_P\\ u_M\\ T_{g,d} \end{bmatrix}}_{\mathbf{u}}
\tag{7}
$$

with

$$
\begin{aligned}
a_{12} &= \frac{1}{J_r}\,f_1(\lambda,\beta), \qquad a_{13} = -\frac{\tilde{V}_P}{J_r}\,f_2(\tilde{x}_P), \qquad a_{23} = \frac{\tilde{V}_M}{J_g}\,f_3(\tilde{x}_M)\\
a_{31} &= \frac{\tilde{V}_P}{C_H}\,f_2(\tilde{x}_P), \qquad a_{32} = -\frac{\tilde{V}_M}{C_H}\,f_3(\tilde{x}_M).
\end{aligned}
\tag{8}
$$

Please cite this article as: H. Schulte, E. Gauterin, Fault-tolerant control of wind turbines with hydrostatic transmission using Takagi–Sugeno and sliding mode techniques, Annual Reviews in Control (2015), http://dx.doi.org/10.1016/j.arcontrol.2015.08.003

To get a TS model structure, the functions (8) can be written as

$$f_1(\lambda,\beta) = w_{11}\,\overline{f}_1 + w_{12}\,\underline{f}_1\,, \qquad f_2(\tilde{x}_P) = w_{21}\,\overline{f}_2 + w_{22}\,\underline{f}_2\,,$$
$$f_3(\tilde{x}_M) = w_{31}\,\overline{f}_3 + w_{32}\,\underline{f}_3 \tag{9}$$

where $\overline{f}_j := \max f_j$ and $\underline{f}_j := \min f_j$. The weighting functions w_{j1} and w_{j2} are defined by

$$w_{j1} = \frac{f_j - \underline{f}_j}{\overline{f}_j - \underline{f}_j}\,, \qquad w_{j2} = \frac{\overline{f}_j - f_j}{\overline{f}_j - \underline{f}_j} \tag{10}$$

which fulfill the convexity condition

$$w_{j1}, w_{j2} \geq 0\,, \quad w_{j1} + w_{j2} = 1 \quad \text{for} \quad j = 1,\ldots,N_l\,, \tag{11}$$

where $N_l = 3$ denotes the number of different nonlinearities in the state space model (4). The membership functions of the TS model are defined by

$$\sum_{i=1}^{N_r} h_i(\mathbf{x},v) = \prod_{j=1}^{N_l=3} (w_{j1} + w_{j2}) \tag{12}$$

with $N_r = 2^{N_l}$ as the number of linear sub-models and result from N_r combinations of the product

$$h_i(\mathbf{x},v) = w_{1k}\cdot w_{2k}\cdot w_{3k} \tag{13}$$

with $k = 1, 2$. Now, it is straightforward to get the TS form of (4) by the substitution of (8) with (9):

$$\dot{\mathbf{x}} = \sum_{i=1}^{8} h_i(\mathbf{z})\,\mathbf{A}_i\,\mathbf{x} + \mathbf{B}\,\mathbf{u}\,, \qquad \mathbf{y} = \mathbf{C}\,\mathbf{x} \tag{14}$$

with $\mathbf{z} = [\ f_1\,,\ f_2\,,\ f_3\ ]^T$, where

$$\mathbf{A}_i = \begin{bmatrix} 0 & a_{12,i} & a_{13,i} & 0 & 0 & 0 \\ 0 & 0 & a_{23,i} & -\frac{1}{J_g} & 0 & 0 \\ a_{31,i} & a_{32,i} & -\frac{k_{leak}}{C_H} & 0 & 0 & 0 \\ 0 & 0 & 0 & -\frac{1}{\tau_g} & 0 & 0 \\ 0 & 0 & 0 & 0 & -\frac{1}{\tau_{x_P}} & 0 \\ 0 & 0 & 0 & 0 & 0 & -\frac{1}{\tau_{x_M}} \end{bmatrix}$$

with

$$a_{12} = \frac{1}{J_r}\,\{\overline{f}_1, \underline{f}_1\}\,, \qquad a_{13} = -\frac{\tilde{V}_P}{J_r}\,\{\overline{f}_2, \underline{f}_2\}\,,$$
$$a_{23} = \frac{\tilde{V}_M}{J_g}\,\{\overline{f}_3, \underline{f}_3\} \qquad a_{31} = \frac{\tilde{V}_P}{C_H}\,\{\overline{f}_2, \underline{f}_2\},$$
$$a_{32} = -\frac{\tilde{V}_M}{C_H}\,\{\overline{f}_3, \underline{f}_3\}\,. \tag{15}$$

2.3. Model uncertainties and disturbances

The main sources of uncertainty in the proposed control-oriented model are the unmodeled dependencies of the leakage flow rate in the hydraulic components, the lack of dynamic inflow and the dynamic stall in the aero map C_Q. The leakage flow rate is linearly correlated with the pressure difference Δp, where the uncertainties are described by an uncertain parameter. Hence, the leakage coefficient in (4) is divided into a nominal value $k_{leak,\,n}$ and an uncertainty Δk_{leak}

$$k_{leak} = k_{leak,n} + \Delta k_{leak}\,. \tag{16}$$

The uncertainty caused by the dynamic inflow and dynamic stall is taken into account by

$$C_Q(\lambda,\beta) = C_{Q,n}(\lambda,\beta)\left(1 + \underbrace{\frac{\Delta C_{Q,n}(\lambda,\beta)}{C_{Q,n}(\lambda,\beta)}}_{\delta_{C,Q}}\right) \tag{17}$$

with the nominal aero map $C_{Q,n}$ and the degree of aerodynamic uncertainty $\delta_{C,\,Q}$.

3. Nominal baseline controller

3.1. Controller structure

Before the fault-tolerant control is considered, we first define the objectives of the fault-free baseline controller design:

1. The rotor/generator speed ratio must be continuously adjusted by the hydrostatic transmission in such a way, that the synchronous generator speed is kept constant independent of the fluctuating wind speed and thus varying rotor speed.
2. In the partial load, the demanded generator torque is controlled deterministically using a look-up table. After reaching the cut-in rotor speed $\omega_{r,cut-in}$, the generator is switched to the grid and the demanded torque is ramped up linearly until the demanded torque is adjusted by the square law

$$T_{g,d}(t) = k_{opt}\,\frac{\omega_r^2(t)}{r_{cv}(t)} \tag{18}$$

with the coefficient k_{opt} to follow the optimal torque, such that the rotor is constantly running around the optimal tip speed ratio (Burton, Jenkins, Sharpe, & Bossanyi, 2011). In the whole partial load region, the pitch angle is kept at a constant value of $\beta = 0°$.

To achieve the first objective, a two-stage adjustment of the pump and motor displacement is pursued. For this, based on (3) the demanded transmission $r_{cv,\,d}$ sets the feed-forward adjustment of the pump and motor displacement with

$$\tilde{x}_{P,d}(t) = \begin{cases} \dfrac{\tilde{V}_M}{\tilde{V}_P}\,r_{cv,d}(t) & \text{if } r_{cv,d}(t) \leq \dfrac{\tilde{V}_P}{\tilde{V}_M} \\ 1 & \text{if } r_{cv,d}(t) > \dfrac{\tilde{V}_P}{\tilde{V}_M} \end{cases}$$
$$\tilde{x}_{M,d}(t) = \begin{cases} 1 & \text{if } r_{cv,d}(t) \leq \dfrac{\tilde{V}_P}{\tilde{V}_M} \\ \dfrac{\tilde{V}_P}{\tilde{V}_M}\,\dfrac{1}{r_{cv,d}(t)} & \text{if } r_{cv,d}(t) > \dfrac{\tilde{V}_P}{\tilde{V}_M} \end{cases} \tag{19}$$

where $\tilde{x}_{P,d} =: u_P$ and $\tilde{x}_{M,d} =: u_M$ denote the controllable inputs of the hydrostatic transmission, see (4). The demanded transmission ratio itself is calculated by the measured rotor speed ω_r and the nominal generator speed $\omega_{g,\,N}$:

$$r_{cv,d}(t) = \omega_{g,N}\,\frac{1}{\omega_r(t)} \qquad \text{with} \qquad \omega_r \geq \omega_{r,cut-in}\,, \tag{20}$$

where $\omega_{g,\,N}$ denotes the nominal mechanical angular speed of the generator. Typically, below the cut-in rotor speed, rotates the turbine in load-free operation (Burton et al., 2011). In addition to the feed-forward path to reach an ideal steady-state response with respect to model uncertainties a feedback path is introduced with a PI controller. For a better understanding the overall control scheme is shown in Fig. 2.

To fulfill the second control objective a torque control is integrated into the control scheme, where the counter torque of the rotor is directly adjusted by a frequency converter of the stator side of the generator. This is a temporary solution, because in a subsequent work this will be replaced by the pressure control of the hydraulic circuit, whereby the converter is no longer required.

Please cite this article as: H. Schulte, E. Gauterin, Fault-tolerant control of wind turbines with hydrostatic transmission using Takagi–Sugeno and sliding mode techniques, Annual Reviews in Control (2015), http://dx.doi.org/10.1016/j.arcontrol.2015.08.003

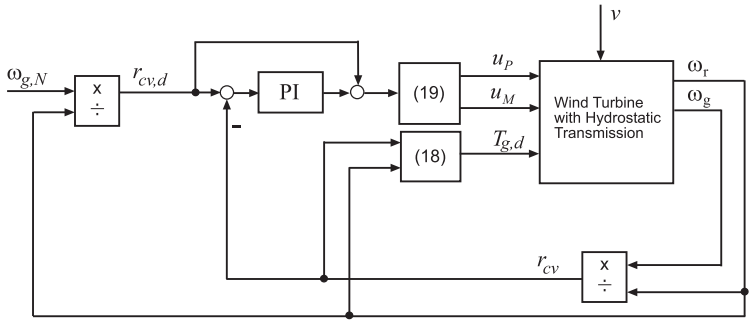

Fig. 2. Structure of the baseline controller for hydrostatic drive trains.

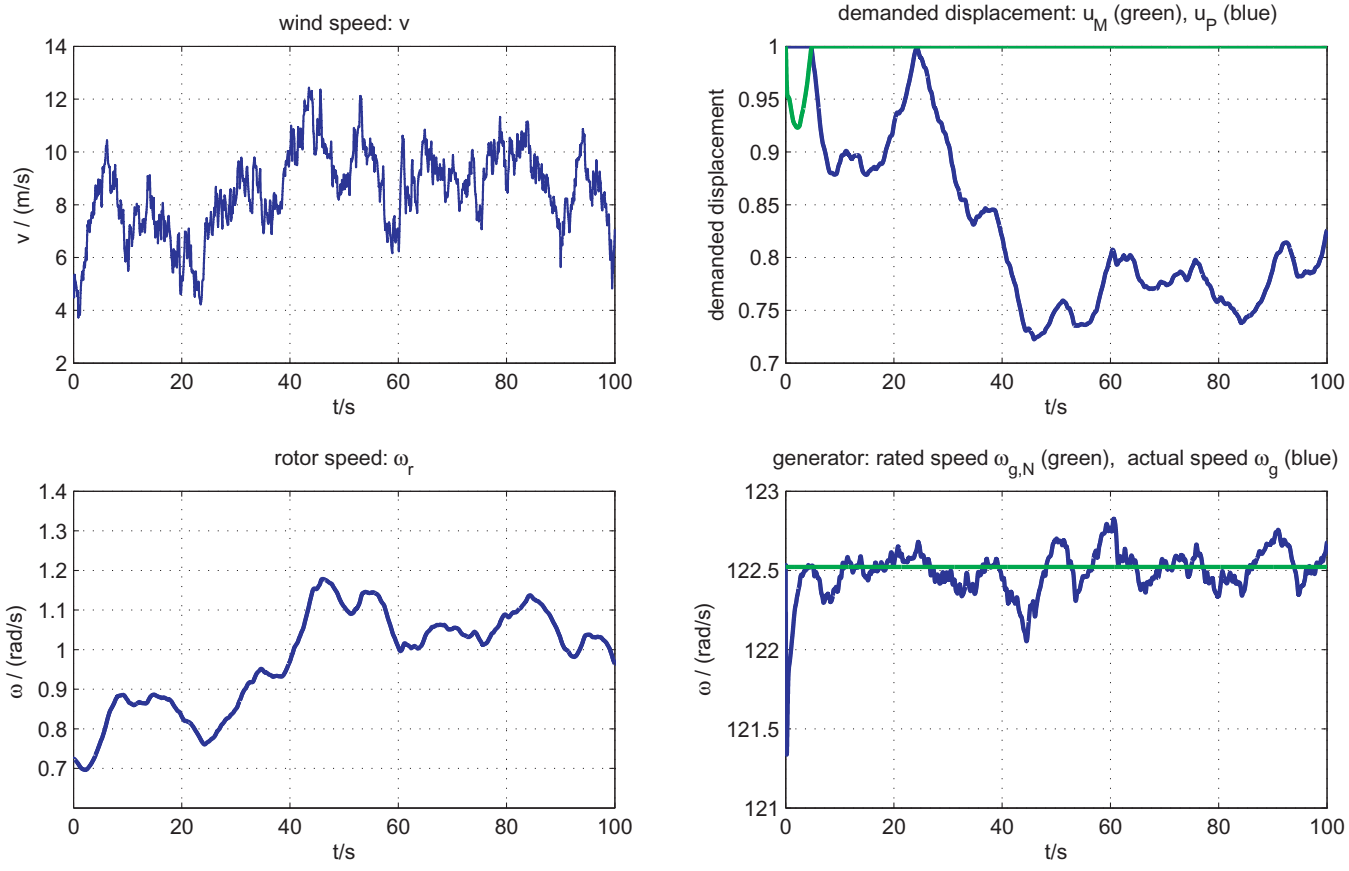

Fig. 3. Nominal simulation with the plant model (4), the baseline controller of Fig. 2 and with turbulent wind speed.

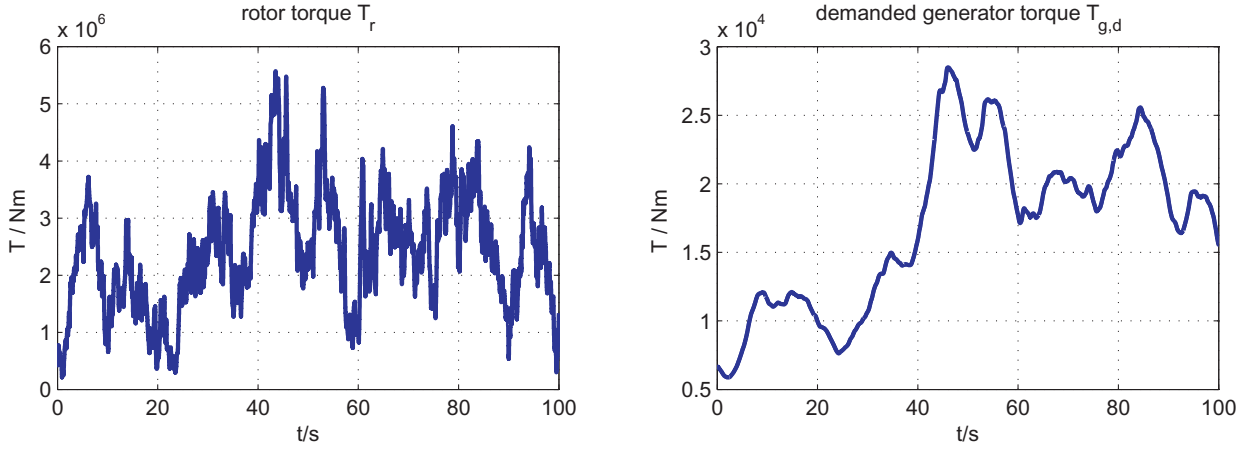

Fig. 4. Nominal simulation of the rotor torque T_r and demanded generator torque $T_{g,d}$.

Please cite this article as: H. Schulte, E. Gauterin, Fault-tolerant control of wind turbines with hydrostatic transmission using Takagi–Sugeno and sliding mode techniques, Annual Reviews in Control (2015), http://dx.doi.org/10.1016/j.arcontrol.2015.08.003

3.2. Illustrative simulation

The simulation of the closed loop dynamics with a turbulent wind speed (turbulence intensity 15%) without actuator faults is shown in Figs. 3 and 4. Here, it can be seen, that the baseline controller and the two-stage pump/motor displacement (19) is able to keep the generator speed to the rated speed $\omega_{g,N} = 122.5$ rad/s during a rotor angular speed variation between 0.7 and 1.2 rad/s.

4. Fault tolerant control scheme

In this section, the fault-tolerant control scheme for actuator fault compensation in wind turbines with hydrostatic transmission are investigated and tested in simulations. The faults are reconstructed by means of a modified TS sliding mode observer. The reconstructed faults are utilized to correct the faulty control input signals, respectively. In this way, virtual actuators are obtained which correspond to the fault-free cases in case of perfect fault reconstruction.

4.1. TS sliding mode observer design

For fault reconstruction by sliding mode observation we consider a norm-bounded uncertain TS model structure:

$$\begin{aligned}\dot{\mathbf{x}} &= \sum_{i=1}^{N_r} h_i(\mathbf{z}) \left(\mathbf{A}_i \mathbf{x} + \mathbf{B}_i \mathbf{u} + \mathbf{F}_i \mathbf{f}_a\right), \\ \mathbf{y} &= \mathbf{C}\mathbf{x}, \end{aligned} \tag{21}$$

where $\mathbf{F}_i \in \mathbb{R}^{n\times a}$ denotes the fault distribution matrix and the faults are presented by $\mathbf{f}_a \in \mathbb{R}^a$. The common $\mathbf{C}$ in (21) is only a small restriction, since many applications e.g. (Georg et al., 2012; Kroll & Schulte, 2014; Schulte & Gerland, 2010) comprise outputs that are linear in the system states. For a stable observer design, three *existence conditions* have to be fulfilled (Edwards & Spurgeon, 1998; Gerland, Groß, Schulte, & Kroll, 2010a, 2010b):

- Condition 1: The faults presented in (21) are unknown but norm bounded by known positive constants $\Xi_{f_a} \in \mathbb{R}^q$ which satisfy $\|\mathbf{f}_a(t)\| \leq \Xi_{f_a}$. Moreover, the system states and inputs are assumed to be bounded.
- Condition 2: Let $q_i = q\ \forall i$ be defined as the number of columns of $\mathbf{F}_i$. Then the condition $q = \text{rank}(\mathbf{C}\mathbf{F}_i) = \text{rank}(\mathbf{F}_i)$ must be fulfilled and it must hold that $p > q$, where p is the number of measurable system states.
- Condition 3: All invariant zeros of $(\mathbf{A}_i, \mathbf{F}_i, \mathbf{C})$ must lie in the open left half of the complex plane.

The design of a sliding mode observer for fault reconstruction applicable for the class of TS systems (21) is carried out in a special canonical form. With a series of transformations $\mathbf{T}_i = \mathbf{T}_{L,i}\,\mathbf{T}_{b,i}\,\mathbf{T}_c$ for each sub-model the TS system is brought into structure where, first, the last p states of the systems are the outputs $\mathbf{y}$ and, second, the faults $\mathbf{f}_a$ only act on the measurable system states (for further details such as the description of the transformation matrices and proofs see (Edwards & Spurgeon, 1998; Georg, 2015; Gerland et al., 2010a)).

The TS model in canonical form is given by

$$\begin{aligned}\dot{\mathbf{x}}_1 &= \sum_{i=1}^{N_r} h_i(\mathbf{z}) \left(\mathcal{A}_{11,i}\,\mathbf{x}_1 + \mathcal{A}_{12,i}\,\mathbf{y} + \mathcal{B}_{1,i}\,\mathbf{u}\right), \\ \dot{\mathbf{y}} &= \sum_{i=1}^{N_r} h_i(\mathbf{z}) (\mathcal{A}_{21,i}\mathbf{x}_1 + \mathcal{A}_{22,i}\mathbf{y} + \mathcal{B}_{2,i}\,\mathbf{u} + \mathcal{F}_{2,i}\mathbf{f}_a), \end{aligned} \tag{22}$$

with the non-measurable states $\mathbf{x}_1 \in \mathbb{R}^{(n-p)}$ and the measurable states $\mathbf{y} \in \mathbb{R}^p$. The transformed system matrices in (22) have the following block structures

$$\mathcal{A}_i = \mathbf{T}_i\,\mathbf{A}_i\,\mathbf{T}_i^{-1} = \begin{bmatrix}\mathcal{A}_{11,i} & \mathcal{A}_{12,i} \\ \mathcal{A}_{21,i} & \mathcal{A}_{22,i}\end{bmatrix}, \quad \mathcal{B}_i = \mathbf{T}_i\,\mathbf{B}_i = \begin{bmatrix}\mathcal{B}_{1,i}^{\mathrm{T}} & \mathcal{B}_{2,i}^{\mathrm{T}}\end{bmatrix}^{\mathrm{T}},$$
$$\mathcal{F}_i = \mathbf{T}_i\,\mathbf{F}_i = \begin{bmatrix}\mathbf{0}^{\mathrm{T}} & \mathcal{F}_{2,i}^{\mathrm{T}}\end{bmatrix}^{\mathrm{T}}.$$

The TS sliding mode (TS SM) observer for the system (22) in transformed form is given by

$$\begin{aligned}\dot{\hat{\mathbf{x}}}_1 &= \sum_{i=1}^{N_r} h_i(\mathbf{z}) \left(\mathcal{A}_{11,i}\,\hat{\mathbf{x}}_1 + \mathcal{A}_{12,i}\,\hat{\mathbf{y}} + \mathcal{B}_{1,i}\,\mathbf{u} - \mathcal{A}_{12,i}\mathbf{e}_y\right), \\ \dot{\hat{\mathbf{y}}} &= \sum_{i=1}^{N_r} h_i(\mathbf{z}) \left(\mathcal{A}_{21,i}\,\hat{\mathbf{x}}_1 + \mathcal{A}_{22,i}\,\hat{\mathbf{y}} + \mathcal{B}_{2,i}\,\mathbf{u} - (\mathcal{A}_{22,i} - \mathcal{A}_{22}^s)\mathbf{e}_y + \boldsymbol{\nu}\right), \end{aligned} \tag{23}$$

where $\mathbf{e}_y = \hat{\mathbf{y}} - \mathbf{y}$ denotes the error vector and $\mathcal{A}_{22}^s$ is a common stable design matrix. An obvious choice for $\mathcal{A}_{22}^s$ is a diagonal matrix where the elements are the desired eigenvalues of the output error dynamics. Using the inverse transformation $\mathbf{T}_i$, the TS sliding mode observer can be obtained in the coordinates $\mathbf{x}$ of the original model (21)

$$\dot{\hat{\mathbf{x}}} = \sum_{i=1}^{N_r} h_i(\mathbf{z}) \left(\mathbf{A}_i\,\hat{\mathbf{x}} + \mathbf{B}_i\,\mathbf{u} - \mathbf{G}_{l,i}\,\mathbf{e}_y + \mathbf{G}_{n,i}\,\boldsymbol{\nu}\right) \tag{24}$$

with the observer gains

$$\mathbf{G}_{l,i} = \mathbf{T}_i^{-1}\begin{bmatrix}\mathcal{A}_{12,i} \\ \mathcal{A}_{22,i} - \mathcal{A}_{22}^s\end{bmatrix} \quad \text{and} \quad \mathbf{G}_{n,i} = \mathbf{T}_i^{-1}\begin{bmatrix}\mathbf{0}_{(n-p)\times p} \\ \mathbf{I}_p\end{bmatrix}.$$

The discontinuous term $\boldsymbol{\nu}$ is necessary to establish and maintain a sliding motion. The sliding motion is given by

$$\boldsymbol{\nu} = -\rho\,\frac{\mathbf{P}_2\,\mathbf{e}_y}{\|\mathbf{P}_2\mathbf{e}_y\|}, \text{ if } \mathbf{e}_y \neq \mathbf{0}, \tag{25}$$

where ρ is a gain factor and $\mathbf{P}_2$ is the symmetric, positive definite solution of the Lyapunov equation

$$\mathbf{P}_2\,\mathcal{A}_{22}^s + \mathcal{A}_{22}^{s\,T}\,\mathbf{P}_2 = -\mathbf{Q}_2, \tag{26}$$

where $\mathbf{Q}_2$ is a symmetric positive definite design matrix. Note that the discontinuous term $\boldsymbol{\nu}$ in (25) is undefined in the case of $\mathbf{e}_y = \mathbf{0}$. Once the sliding surface

$$\mathcal{S} = \{\mathbf{e}(t) \in \mathbb{R}^n := \mathcal{C}\,\underbrace{[\,\mathbf{e}_1^{\mathrm{T}}\ \mathbf{e}_y^{\mathrm{T}}\,]^{\mathrm{T}}}_{\mathbf{e}} = \mathbf{0}\} \tag{27}$$

$$\text{with} \quad \mathcal{C} = \mathbf{C}\,\mathbf{T}_c^{-1} = \begin{bmatrix}\mathbf{0}_{p\times(n-p)}\ \mathbf{I}_p\end{bmatrix} \tag{28}$$

is reached at the time $t = t_r$, the TS SM observer attempts to maintain the sliding motion on the surface $\mathcal{S}$.

4.2. Actuator fault reconstruction

For the actuator fault reconstruction we consider first the TS model (22) and the TS SM observer (23) in canonical form. By the substitution of $\dot{\mathbf{e}}_1 = \dot{\hat{\mathbf{x}}}_1 - \dot{\mathbf{x}}_1$ and $\dot{\mathbf{e}}_y = \dot{\hat{\mathbf{y}}} - \dot{\mathbf{y}}$ with (22), (23) it can be verified that

$$\dot{\mathbf{e}}_1 = \sum_{i=1}^{N_r} h_i(\mathbf{z})\mathcal{A}_{11,i}\,\mathbf{e}_1 \tag{29}$$

and

$$\dot{\mathbf{e}}_y = \sum_{i=1}^{N_r} h_i(\mathbf{z})\left(\mathcal{A}_{21,i}\,\mathbf{e}_1 + \mathcal{A}_{22}^s\,\mathbf{e}_y + \boldsymbol{\nu} - \mathcal{F}_{2,i}\,\mathbf{f}_a\right). \tag{30}$$

Please cite this article as: H. Schulte, E. Gauterin, Fault-tolerant control of wind turbines with hydrostatic transmission using Takagi–Sugeno and sliding mode techniques, Annual Reviews in Control (2015), http://dx.doi.org/10.1016/j.arcontrol.2015.08.003

Assume the TS SM observer has been designed and a sliding motion has been established from $t \geq t_r$. This means that $\mathbf{e}_y = \mathbf{0}$, $\dot{\mathbf{e}}_y = \mathbf{0}$ and in this case the error equation (30) is simplified to

$$\mathbf{0} = \sum_{i=1}^{N_r} h_i(\mathbf{z}) \left(\mathcal{A}_{21,i}\, \mathbf{e}_1 + \boldsymbol{\nu}_{eq} - \mathcal{F}_{2,i}\, \mathbf{f}_a \right) \tag{31}$$

and the discontinuous term $\boldsymbol{\nu}$ is replaced by the so-called equivalent output injection signal (Edwards & Spurgeon, 1998)

$$\boldsymbol{\nu}_{eq} = \boldsymbol{\nu}_\delta (t \geq t_r) \,, \tag{32}$$

where $\boldsymbol{\nu}_\delta$ denotes an approximation of (25) by introducing a small positive scalar δ

$$\boldsymbol{\nu}_\delta = -\rho \, \frac{\mathbf{P}_2\, \mathbf{e}_y}{\|\mathbf{P}_2 \mathbf{e}_y\| + \delta} \,. \tag{33}$$

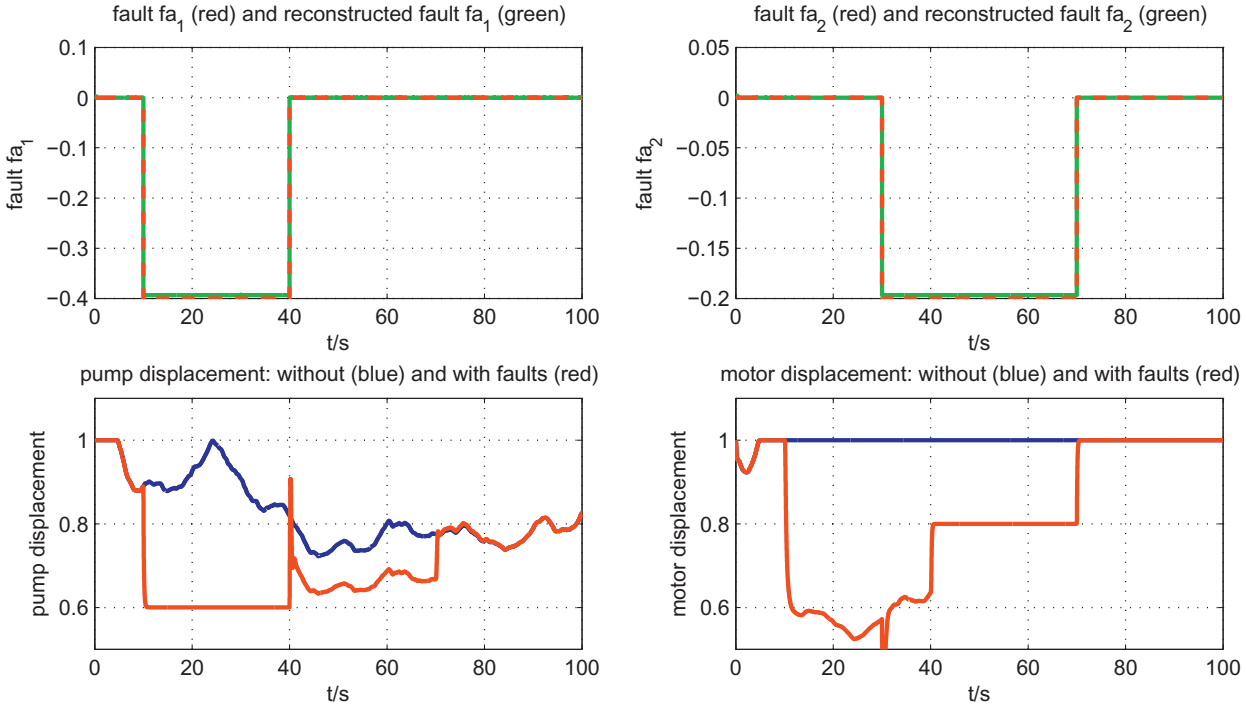

Fig. 5. Actual actuator offset faults $\mathbf{f}_a$ ($f_{a,1} = -0.4$, $f_{a,2} = -0.2$), reconstructed actuator faults $\hat{\mathbf{f}}_a$ and the impact on the actual pump $\tilde{x}_P$ and motor displacement $\tilde{x}_M$ using the baseline controller (Fig. 2).

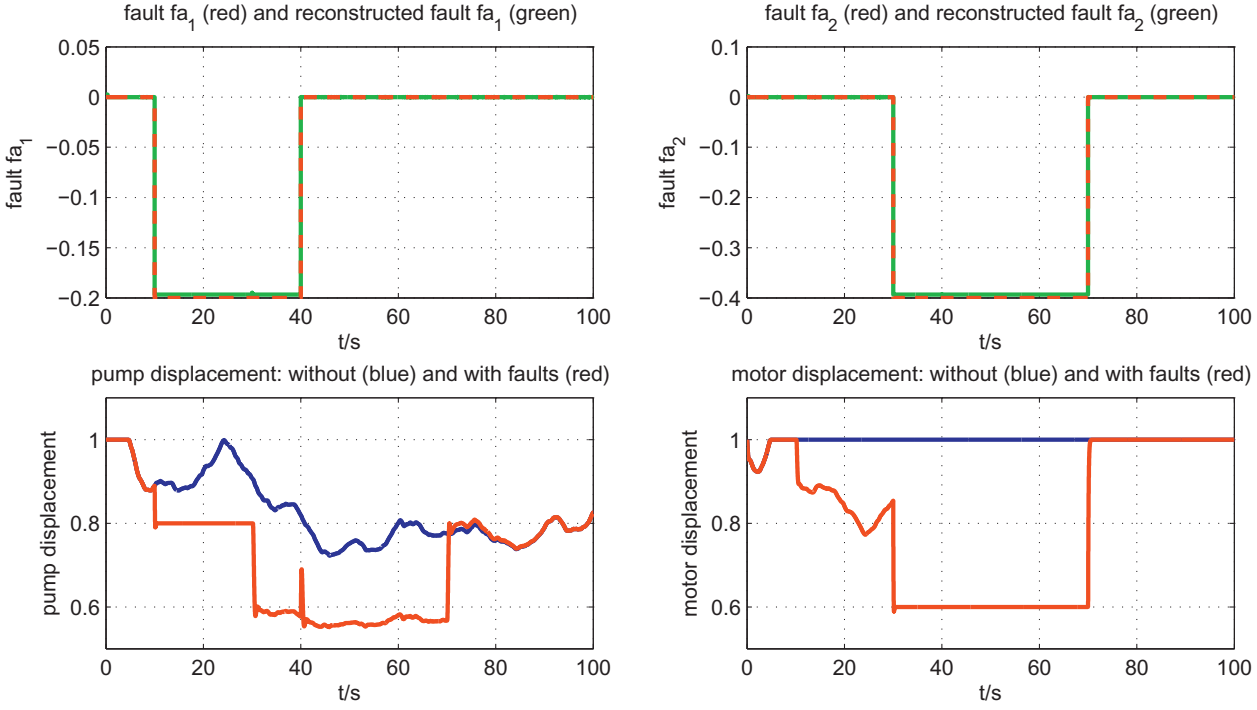

Fig. 6. Actual actuator offset faults $\mathbf{f}_a$ ($f_{a,1} = -0.2$, $f_{a,2} = -0.4$), reconstructed actuator faults $\hat{\mathbf{f}}_a$ and the impact on the actual pump $\tilde{x}_P$ and motor displacement $\tilde{x}_M$ using the baseline controller (Fig. 2).

Please cite this article as: H. Schulte, E. Gauterin, Fault-tolerant control of wind turbines with hydrostatic transmission using Takagi–Sugeno and sliding mode techniques, Annual Reviews in Control (2015), http://dx.doi.org/10.1016/j.arcontrol.2015.08.003

It should be noted that the value of δ should be chosen as small as possible, because it influence the quality of the fault reconstruction. Thus, the equivalent output injection signal is given by rearranging Eq. (31)

$$\boldsymbol{v}_{eq} = \sum_{i=1}^{N_r} h_i(\mathbf{z})\left(\mathcal{F}_{2,i}\,\mathbf{f}_a - \mathcal{A}_{21,i}\,\mathbf{e}_1\right). \tag{34}$$

Substituting the steady state solution of (29) into (34) we get the relation

$$\mathbf{f}_a = \left[\sum_{i=1}^{N_r} h_i(\mathbf{z})\;\mathcal{F}_{2,i}\right]^{+} \boldsymbol{v}_{eq}, \tag{35}$$

where $(\,\cdot\,)^{+}$ denotes the pseudo-inverse of the convex combination of the matrices $\mathcal{F}_{2,i}$. Note the pseudo-inverse of the convex combination of matrices exists if the full rank characterization is satisfied by the theorem proposed in Kolodziejczak and Szulc (1999).

4.2.1. Fault tolerant control

If faults occur in the system, provided that these faults can be accurately reconstructed, the most straightforward strategy to achieve fault-tolerance is a fault compensation method, whereby the reconstructed and possibly filtered faults are subtracted from the demanded control input:

$$\mathbf{u}_{\text{corr}} = \mathbf{u} - \hat{\mathbf{f}}_{a,\text{filt}}, \tag{36}$$

where first order delay filters can be used to avoid feeding back erroneous peaks into the fault-tolerant control scheme. The dynamics of the filtered reconstructed fault signals is given by (Georg, 2015)

$$\dot{\hat{\mathbf{f}}}_{a,\text{filt}} = -\text{diag}(\,1/\tau_1 \cdots 1/\tau_q\,)\,\hat{\mathbf{f}}_{a,\text{filt}} + \text{diag}(\,1/\tau_1 \cdots 1/\tau_q\,)\,\hat{\mathbf{f}}_a, \tag{37}$$

where $1/\tau_1 \ldots 1/\tau_q$ denote the delay time constants. After applying the correction (36), the actual input signal $\tilde{\mathbf{u}}$ that acts on the system

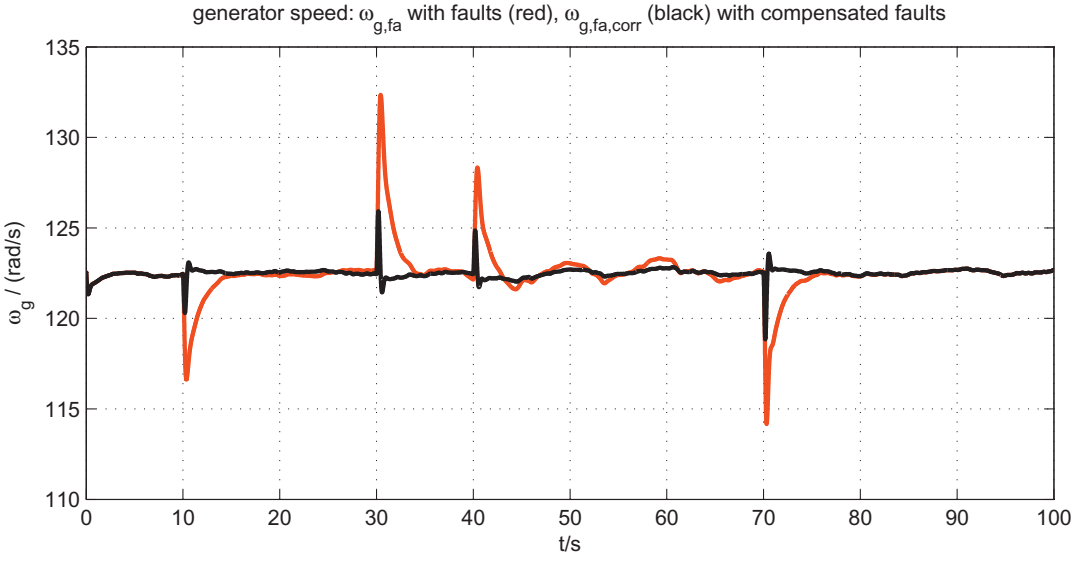

Fig. 7. Impact of the actuator faults (Fig. 6) on the actual generator speed ω_g without (red line) and with fault compensation (black line). (For interpretation of the references to color in this figure legend, the reader is referred to the web version of this article.)

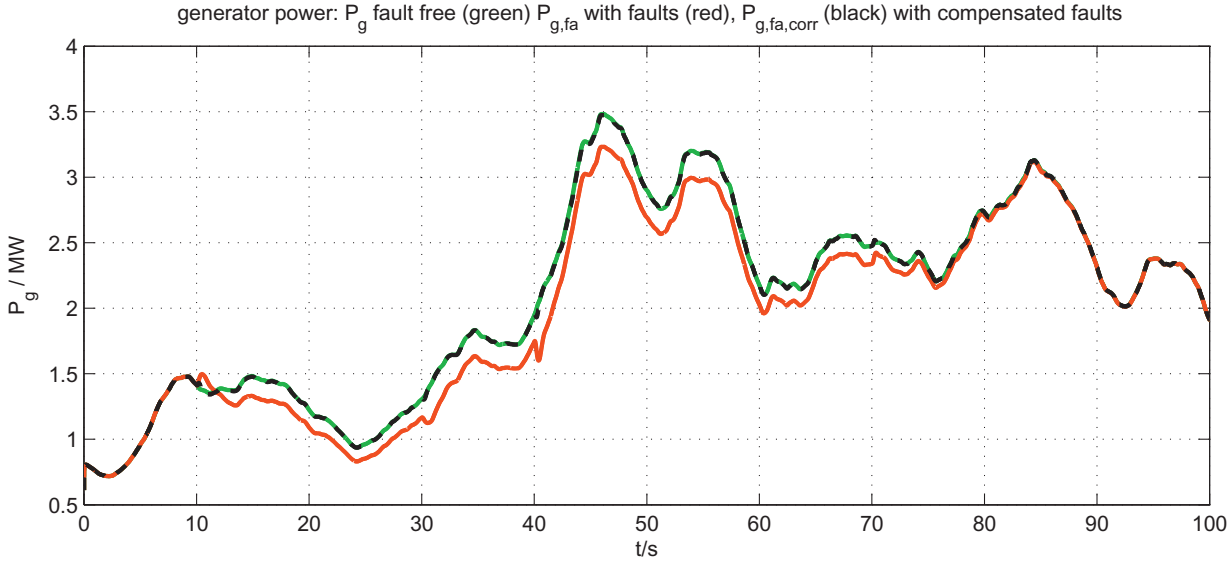

Fig. 8. Impact of the actuator faults (Fig. 6) on the generator output power P_g without fault (green line), with fault (red line) and with fault compensation (black dashed line). (For interpretation of the references to color in this figure legend, the reader is referred to the web version of this article.)

Please cite this article as: H. Schulte, E. Gauterin, Fault-tolerant control of wind turbines with hydrostatic transmission using Takagi–Sugeno and sliding mode techniques, Annual Reviews in Control (2015), http://dx.doi.org/10.1016/j.arcontrol.2015.08.003

is given by

$$\tilde{\mathbf{u}} = \mathbf{u}_{\text{corr}} + \mathbf{f}_a = \underbrace{\mathbf{u} - \hat{\mathbf{f}}_{a,\text{filt}}}_{\mathbf{u}_{\text{corr}}} + \mathbf{f}_a \,. \tag{38}$$

It is clear that the quality of the fault compensation depends on the quality of the fault reconstruction. If $\hat{\mathbf{f}}_{a,\text{filt}}$ were a perfect reconstruction of $\mathbf{f}_a$, $\tilde{\mathbf{u}}$ would exactly correspond to the original faultless control signal $\mathbf{u}$.

4.3. Illustrative simulation

As an illustrative case study, first, the impact of two partly temporally superimposed actuator faults are simulated with the model equation (7) and the baseline controller (Fig. 2). The additive fault signal on the input u_P denoted as $f_{a,1}$ and on the input u_M denoted as $f_{a,2}$ are illustrated in Figs. 5 and 6.

For the reconstruction of the actuator faults $\mathbf{f}_a = [\, f_{a,1}\,,\, f_{a,2}\,]^T$, a TS sliding mode observer is designed using the wind turbine model in TS form (14) with the observer states $\mathbf{x} = [\, \omega_r \quad \omega_g \quad \Delta p \quad T_g \quad \tilde{x}_P \quad \tilde{x}_M\,]^T$ and the measurable signals $\mathbf{y} = [\, \omega_r \quad \omega_g \quad T_g \quad \tilde{x}_P \quad \tilde{x}_M\,]^T$. As the faults are modeled by additive offsets, there is only one common actuator fault matrix $\mathbf{F}$ in the uncertain TS model structure (21), which is equal to the input matrix $\mathbf{B}$ (14).

The following observer parameters were used

$$\mathcal{A}_{22}^s = \text{diag}(-20 \cdots -20)\,, \qquad \rho = 100\,, \qquad \delta = 0.002\,. \tag{39}$$

The reconstructed faults are filtered with (37) to avoid feeding back erroneous peaks into the fault-tolerant control scheme. Here, the delay time constant is set to $\tau_{1,2} = 0.1$ s.

It can be seen from the upper sub-figures in Figs. 5 and 6, that both faults are reasonably well reconstructed. Compared to the simulation results, the discrepancy between the actual and the reconstructed fault values is negligibly small. Furthermore, it can be seen from Fig. 7, that in the faulty case the generator speed deviates strongly from the nominal value. Indeed the PI-controller (Fig. 2) is able to reach the rated speed, but with not allowable overspeed caused by large inertia of the rotor.

However, it can be seen from Figs. 7 and 8 with active fault compensation by (36), the fault free behavior is almost recovered, avoiding the rotor overspeed and the decrease of generator output power that occurs without fault compensation. The small deviations are caused by the error dynamics of the TS SM observer and result from filtering the reconstructed fault signals with (37).

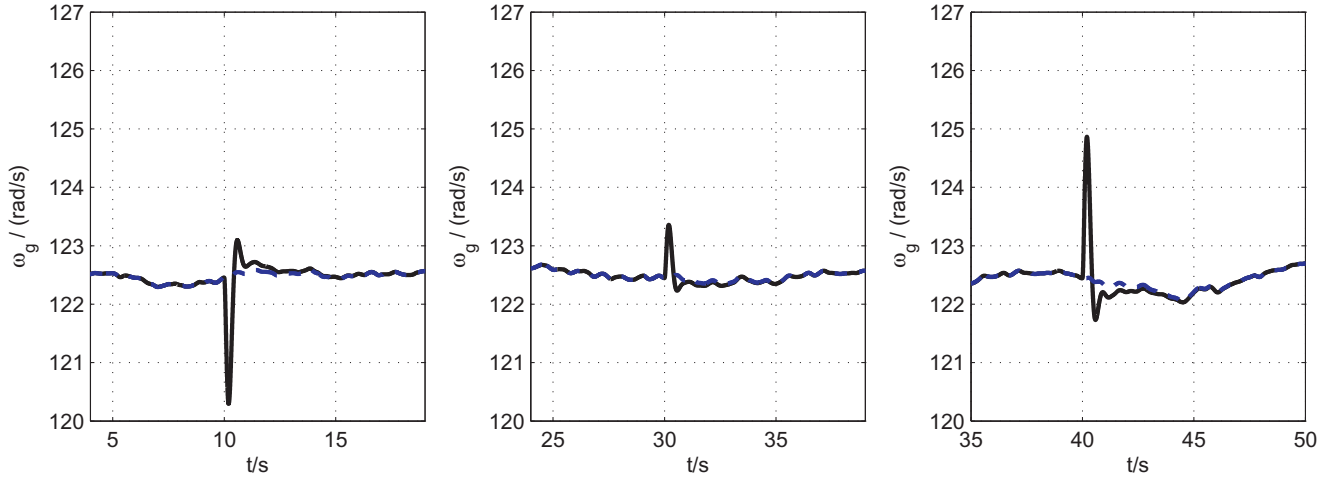

Fig. 9. Actual generator speed: Comparison between the fault free and faulty case ($f_{a,1}(t) = -0.2,\ t \in [10, 40]$; $f_{a,2}(t) = -0.1,\ t \in [30, 70]$) with compensation of actuator faults *without model uncertainties*. The blue line represents the fault free and the black line represents the generator speed with fault compensation. (For interpretation of the references to color in this figure legend, the reader is referred to the web version of this article.)

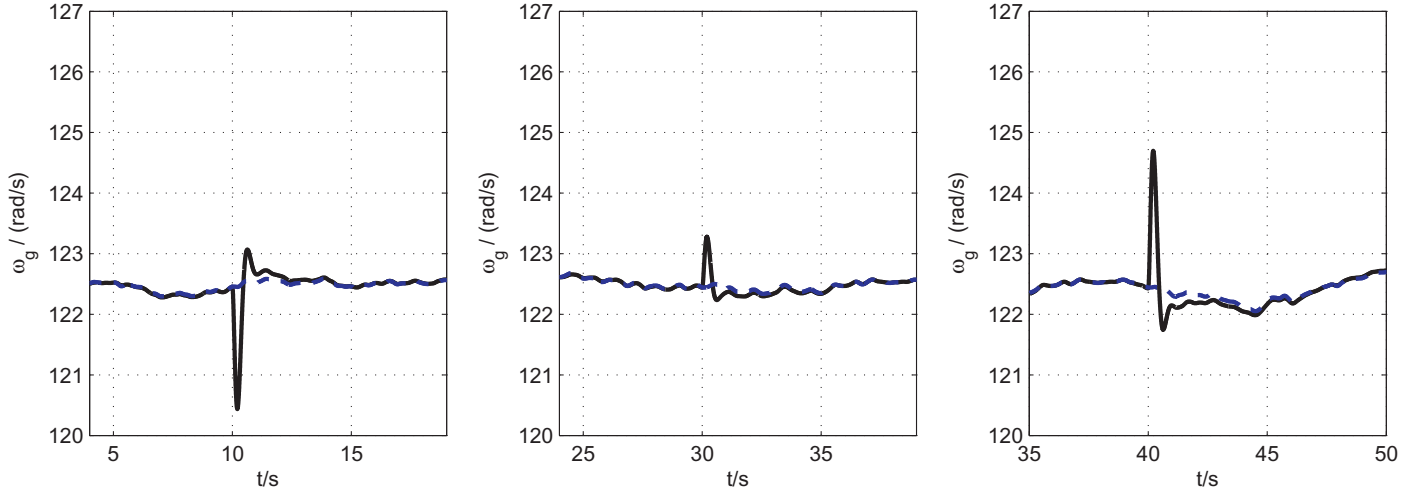

Fig. 10. Actual generator speed: Comparison between the fault free and faulty case ($f_{a,1}(t) = -0.2,\ t \in [10, 40]$; $f_{a,2}(t) = -0.1,\ t \in [30, 70]$) with compensation of actuator faults with respect to *uncertainty in the leakage flow rate* $\Delta k_{leak}/k_{leak} = 0.15$ (16). The blue line represents the fault free and the black line represents the generator speed with fault compensation. (For interpretation of the references to color in this figure legend, the reader is referred to the web version of this article.)

Please cite this article as: H. Schulte, E. Gauterin, Fault-tolerant control of wind turbines with hydrostatic transmission using Takagi–Sugeno and sliding mode techniques, Annual Reviews in Control (2015), http://dx.doi.org/10.1016/j.arcontrol.2015.08.003

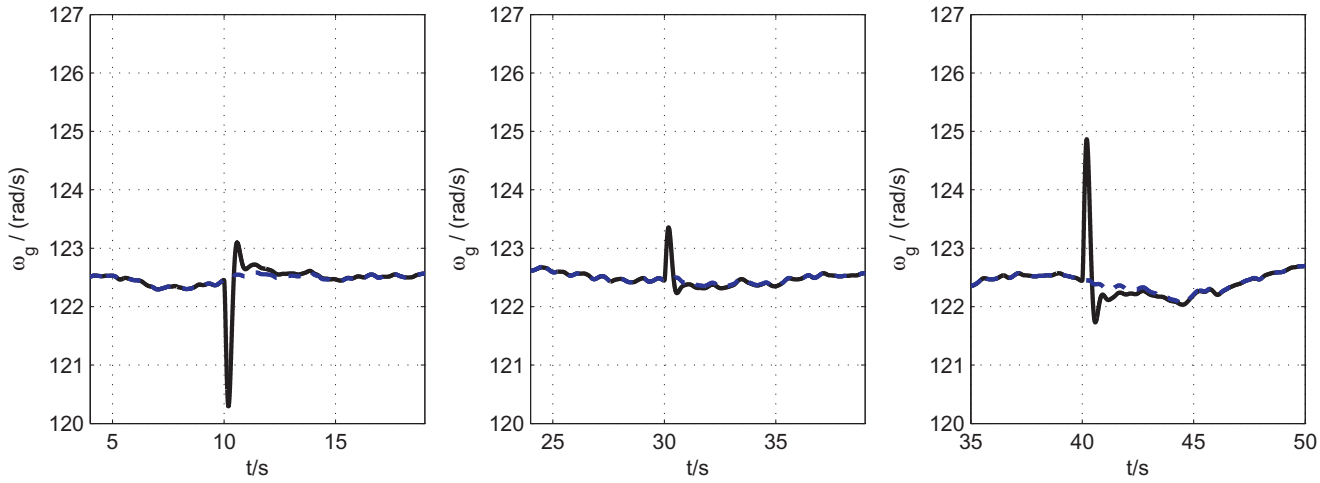

Fig. 11. Actual generator speed: Comparison between the fault free and faulty case ($f_{a,1}(t) = -0.2,\ t \in [10, 40]$; $f_{a,2}(t) = -0.1,\ t \in [30, 70]$) with compensation of actuator faults with respect to *aerodynamic uncertainty* $\delta_{C,Q} = 0.2$ (17). The blue line represents the fault free and the black line represents the generator speed with fault compensation. (For interpretation of the references to color in this figure legend, the reader is referred to the web version of this article.)

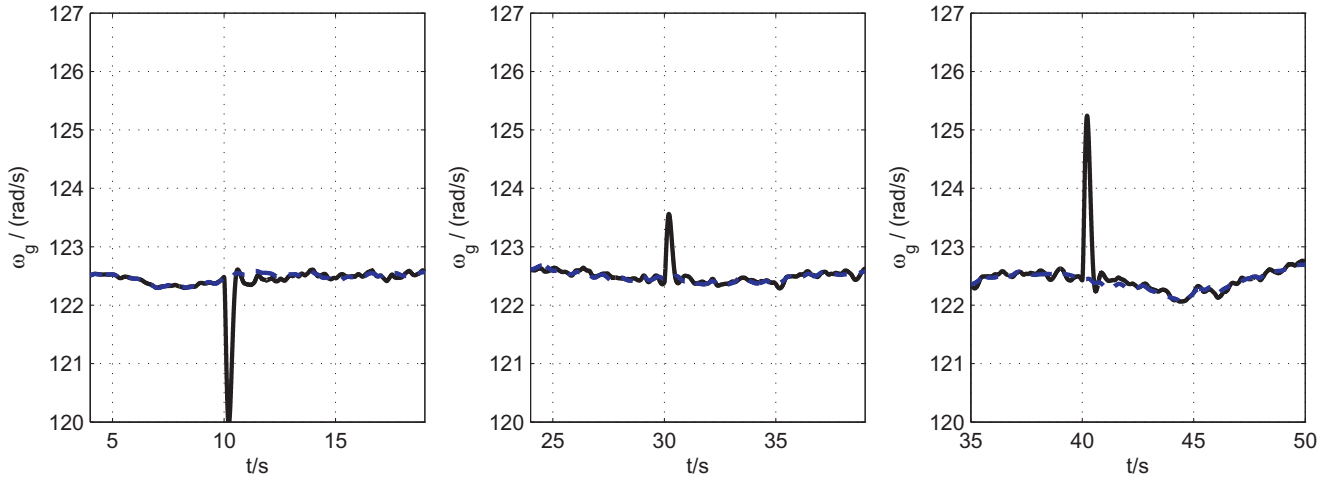

Fig. 12. Actual generator speed: Comparison between the fault free and faulty case ($f_{a,1}(t) = -0.2,\ t \in [10, 40]$; $f_{a,2}(t) = -0.1,\ t \in [30, 70]$) with compensation of actuator faults with respect to *measurement noise* up to $\pm$ 2 %. The blue line represents the fault free and the black line represents the generator speed with fault compensation. (For interpretation of the references to color in this figure legend, the reader is referred to the web version of this article.)

The robustness of the proposed approach is demonstrated by three different case studies. As a comparison Fig. 9 shows the nominal case without uncertainties but with the same additive actuator faults. Fig. 10 shows what happens if the leakage flow rate increases by 15 percent. The robustness against a change of the aerodynamic rotor torque coefficient C_Q is presented in Fig. 11. Finally, the effect of measurement noise up to $\pm$2 percent is depicted in Fig. 12.

4.4. Comparison with other methodologies

In this paper, an FTC scheme for actuator faults in wind turbines with hydrostatic transmission is presented based on direct fault reconstruction by means of a Takagi–Sugeno sliding mode observer. This concept was also applied in Georg, Heyde, and Schulte (2014) to achieve fault-tolerant control in the presence of sensor faults. In Sami and Patton (2014) a direct fault reconstruction by means of a fast adaptive fuzzy estimator, respectively a proportional multiple integral observer are used to achieve a fault-tolerant behavior in the partial load region.

No direct fault reconstruction is implemented in the following works: In Odgaard and Stoustrup (2012), an FTC scheme is set up based on a bank of unknown input observers. However, each single fault scenario requires a different observer design. In In Rotondo, Nejjari, Puig, and Blesa (2012) a parameter estimation scheme is used for obtaining fault estimates, which are then utilized in a virtual actuator/sensor fault-tolerant control strategy. As for FTC solutions using the FAST FDI benchmark model (Badihi et al., 2014; Odgaard & Johnson, 2013) present a Fuzzy Modeling and Identification (FMI) technique, which is applied to achieve FTC. The algorithm requires an initial training with a predefined dataset.

5. Conclusion

In this work, a fault-tolerant control scheme for wind turbines with hydrostatic transmission was investigated based on direct fault reconstruction by means of Takagi–Sugeno sliding mode observers. The precise fault reconstructions allowed for using the signals in fault compensation schemes to achieve fault-tolerant control in the presence of actuator faults with a behavior similar to the fault-free case.

In a future work, the method will be validated with the aeroelastic code FAST similar to the procedure in Georg (2015). This is used primarily to consider the robustness and reliability of the FTC scheme under more realistic conditions before it is applied to current and future wind turbines.

Please cite this article as: H. Schulte, E. Gauterin, Fault-tolerant control of wind turbines with hydrostatic transmission using Takagi–Sugeno and sliding mode techniques, Annual Reviews in Control (2015), http://dx.doi.org/10.1016/j.arcontrol.2015.08.003

References

Badihi, H., Zhang, Y., & Hong, H. (2014). Fuzzy gain-scheduled active fault-tolerant control of a wind turbine. *Journal of the Franklin Institute, 351*(7), 3677–3706.
Badihi, H., Zhang, Y., & Hong, H. (2015). Wind turbine fault diagnosis and fault-tolerant torque load control against actuator faults. *IEEE Transactions on Control Systems Technology, 23*(4), 1351–1372.
Burton, T., Jenkins, N., Sharpe, D., & Bossanyi, E. (2011). *Wind energy handbook* (2nd). John Wiley & Sons, Ltd.
Diepeveen, N., & Laguna, A. (2011). Dynamic modeling of fluid power transmissions for wind turbines. In *Proceedings of the Offshore Wind Energy Conference, EWEA (The European wind energy association)*. Amsterdam, The Netherlands.
Dolan, B., & Aschemann, H. (2012). Control of a wind turbine with a hydrostatic transmission – an extended linearisation approach. In *Proceedings of the 17th international conference on methods and models in automation and robotics (MMAR)*. Miedzyzdroje, Poland.
Edwards, C., & Spurgeon, S. K. (1998). *Sliding mode control: Theory and applications*. Boca Raton: Taylor & Francis.
Georg, S. (2015). *Fault diagnosis and fault-tolerant control of wind turbines nonlinear Takagi-Sugeno and sliding mode techniques*. University Rostock, Fakultät für Maschinenbau und Schiffstechnik Ph.D. thesis..
Georg, S., Heyde, S., & Schulte, H. (2014). Sensor fault-tolerant control of a drivetrain test rig via an observer-based approach within a wind turbine simulation model. *Journal of Physics: Conference Series, 570*, 1–11.
Georg, S., & Schulte, H. (2013). Actuator fault diagnosis and fault-tolerant control of wind turbines using a Takagi-Sugeno sliding mode observer. In *Proceedings of the international conference on control and fault-tolerant systems (SysTol)* (pp. 516–522). Nice, France.
Georg, S., Schulte, H., & Aschemann, H. (2012). Control-oriented modelling of wind turbines using a Takagi-Sugeno model structure. In *Proceedings of the IEEE international conference on fuzzy systems* (pp. 1737–1744). Brisbane, Australia.
Gerland, P., Groß, D., Schulte, H., & Kroll, A. (2010a). Design of sliding mode observers for TS fuzzy systems with application to disturbance and actuator fault estimation. In *Proceedings of the IEEE conference on decision and control* (pp. 4373–4378). Hilton Atlanta Hotel, Atlanta, GA, USA.
Gerland, P., Groß, D., Schulte, H., & Kroll, A. (2010b). Robust adaptive fault detection using global state information and application to mobile working machines. In *Proceedings of the conference on control and fault-tolerant systems* (pp. 813–818). Nice, France.
Kolodziejczak, B., & Szulc, T. (1999). Convex combinations of matrices – full rank characterization. *Linear Algebra and its Applications, 287*, 215–222.
Kroll, A., & Schulte, H. (2014). Benchmark problems for nonlinear system identification and control using soft computing methods: need and overview. *Applied Soft Computing, 25*(12), 496–513.
Odgaard, P., & Johnson, K. (2013). Wind turbine fault detection and fault tolerant control – an enhanced benchmark challenge. In *Proceedings of the American control conference* (pp. 4447–4452). Washington, USA.
Odgaard, P. F., & Stoustrup, J. (2012). Fault tolerant control of wind turbines using unknown input observers. In *Proceedings of the IFAC symposium on fault detection, supervision and safety of technical processes* (pp. 313–318). Mexico City, Mexico.
Odgaard, P. F., Stoustrup, J., & Kinnaert, M. (2009). Fault tolerant control of wind turbines – a benchmark model. In *Proceedings of the IFAC symposium on fault detection, supervision and safety of technical processes* (pp. 155–160). Barcelona, Spain.
Ragheb, A. M., & Ragheb, M. (2010). Wind turbine gearbox technologies. In *Proceedings of the 1st international nuclear & renewable energy conference (INREC)*.
Rotondo, D., Nejjari, F., Puig, V., & Blesa, J. (2012). Fault tolerant control of the wind turbine benchmark using virtual sensors/actuators. In *Proceedings of the IFAC symposium on fault detection, supervision and safety of technical processes* (pp. 114–119). Mexico City, Mexico.
Rotondo, D., Puig, V., Valle, J. M. A., & Nejjari, F. (2013). FTC of LPV Systems using a bank of virtual sensors: Application to wind turbines. In *Proceedings of the international conference on control and fault-tolerant systems (SysTol)* (pp. 492–497). Nice, France.
Sami, M., & Patton, R. J. (2012a). Fault tolerant adaptive sliding mode controller for wind turbine power maximisation. In *Proceedings of the 7th IFAC symposium on robust control design* (pp. 499–504). Aalborg, Denmark.
Sami, M., & Patton, R. J. (2012b). An FTC approach to wind turbine power maximisation via T-S fuzzy modelling and control. In *Proceedings of the IFAC symposium on fault detection, supervision and safety of technical processes* (pp. 349–354). Mexico City, Mexico.
Sami, M., & Patton, R. J. (2014). Active sensor fault tolerant output feedback tracking control for wind turbine systems via T-S model. *Engineering Applications of Artificial Intelligence, 34*, 1–12.
Schulte, H. (2014). Control-oriented description of large scale wind turbines with hydrostatic transmission using Takagi-Sugeno models. In *Proceedings of the IEEE international conference on control applications (CCA)*. Antibes, France.
Schulte, H., & Gerland, P. (2010). Observer-based estimation of pressure signals in hydrostatic transmissions. In *Proceedings of the IFAC symposium advances in automotive control (AAC)*. Munich, Germany.
Simani, S., & Castaldi, P. (2014). Active actuator fault-tolerant control of a wind turbine benchmark model. *International Journal Robust Nonlinear Control, 24*(8–9), 1283–1303.
Skaare, B., Nielsen, F. G., & Hörnsten, B. (2013). Modeling, simulation and control of a wind turbine with a hydraulic transmission system . *Wind Energy, 16*, 1259–1276.
Sloth, C., Esbensen, T., & Stoustrup, J. (2011). Robust and fault-tolerant linear parameter-varying control of wind turbines. *Mechatronics, 21*, 645–659.

Horst Schulte received the diploma degree in Electrical Engineering from TU Berlin and the Ph.D. degree in Control Engineering from University Kassel (Germany). He joined the Bosch Rexroth AG (Bosch Group) in 2005 where he worked in R&D projects in the field of modeling, optimization and advanced control of actuators, power systems and drive trains. Since November 2009, he has been a full Professor at the University of Applied Sciences HTW Berlin. His research interests include nonlinear controller and observer design with Takagi–Sugeno (TS), LPV and sliding-mode techniques, robust control system design, active fault-tolerant control (FTC) system design with industrial applications. Prof. Schulte is one of European Advanced Control and Diagnosis (EACD) steering committee members and a member of IFAC TC 6.4 Fault Detection, Supervision & Safety of Technical Processes and 7.1 Automotive Control.

Eckhard Gauterin received the diploma degree from TU Berlin, Germany, 2005, in mechanical engineering. After graduating he was with two independent engineering companies, dedicated to wind turbine prototype development, working as a design engineer, project manager and managing director for five years. He is currently a research assistant with the Department Engineering I, Control Engineering Group, University of Applied Sciences, Berlin, Germany. He studies control systems and control applications, especially wind energy. Some of his recent wind energy control projects include load reduction on wind turbines using observer based feedforward control.

Please cite this article as: H. Schulte, E. Gauterin, Fault-tolerant control of wind turbines with hydrostatic transmission using Takagi–Sugeno and sliding mode techniques, Annual Reviews in Control (2015), http://dx.doi.org/10.1016/j.arcontrol.2015.08.003